PROCESSING AND PROPERTIES OF FE-10AL-4CR-4Y2O3 OXIDE DISPERSION STRENGTHENED (ODS) ALLOY CONSOLIDATED BY HOT ROTARY SWAGING

[1]Ludmila KRÁTKÁ, [2]Marek BENČ

[1]VSB - Technical University of Ostrava, Ostrava, Czech Republic, EU, ludmila.kratka@vsb.cz

[2]Institute of Physics of Materials of the CAS, Brno, Czech Republic, EU

https://doi.org/10.37904/metal.2022.4400

Abstract

This study deals with new generation of ODS alloys strengthened with a high-volume fraction of Y-nanooxides of 4 %. The ODS alloy is produced using powder metallurgy consisting of mechanical alloying of input powders followed by hot consolidation of canned powder using rotary swaging technology and secondary recrystallization to provoke coarse-grained microstructure. We focus on the microstructure characterization after individual processing steps and measurement of mechanical properties after consolidation and after secondary recrystallization at room temperature and 1100 °C. The mechanical properties of the studied ODS alloy are compared with those of a conventionally produced alloy as INCONEL718.

Keywords: Oxide dispersion strengthened (ODS) alloy, powder hot consolidation, rotary swaging

1. INTRODUCTION

The development of advanced materials that excel in resistance to high temperature creep and oxidation is one of the most challenging goals of materials research today. Ni-based super alloys are applicable up to 1100 °C. Oxide dispersion strengthened ferritic alloys (ODS) are applicable up to 1300 °C. In addition, heavy tungsten alloys (THAs) are used up to 1500 °C. These metallic materials achieve the highest level of strength with low creep under thermal loading [1-3].

Oxide dispersion strengthened (ODS) materials are mainly produced because of their extremely high mechanical and oxidation resistance at high temperatures. They also excel in microstructural stability. Most commonly, a small amount of yttrium (from 0.3 to 0.5 wt%) is added to these alloys and dispersed in the metal matrix. Other oxides such as lanthanum oxides, scandium, cerium are currently being studied as substitutes for Y2O3 [4-6].

Powder metallurgy processes very convenient to incorporate the required amount of oxides into the ODS material. In the first step, powders are prepared by mechanical alloying [7]. Then in the second step, they can be consolidated by several methods such as forging or hot rolling. Rotary swaging (RS) has emerged as a very advantageous technology for consolidation and processing of these materials. Rotary swaging belongs to the methods where intense plastic deformation occurs. This technology is characterized by gradual increments of embedded deformation and high-frequency punches through the matrix. The blank is usually compacted rapidly by rapidly rotating dies at a small diameter. Optimization of the conditions during hot RS, plays an important role in the resulting textured microstructure and consequently in the mechanical properties. Furthermore, the development of residual stresses and packing force, is crucial to obtain a fully compacted bar with minimal heterogeneity. This is very advantageous in the case of powder-based materials [8-11].

2. MATERIAL AND METHODS

Homogeneous Fe-10Al-4Cr-3Y_2O_3 powder was prepared from Fe, Al, Cr and Y_2O_3 powders, which were of 99.9 % purity. These powders were mixed in a custom-made ball mill. The ball mill was filled with bearing

balls and 1 kg of the powder mixture. This mixture was mechanically alloyed under vacuum by rotating the grinding vessel. After sufficient alloying time, a homogeneous solid solution with a high density of defects such as dislocations and vacancies was achieved. The next step was the preparation of a vacuum-sealed container (**Figure 1**) into which the powder was enclosed.

Figure 1 Vacuum tight container with powder mixture

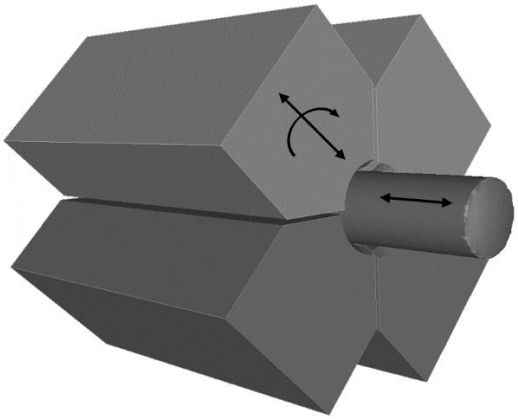

Figure 2 Schematic of rotary swaging

Hot rotary forging technology (**Figure 2**) was used to process the blank. The actual forging was carried out on a rotary forging machine from HMP. The forging temperature was 950 ± 20 °C. The semi-finished product was heated and maintained on a pelot in an atmospheric furnace. Rotary forging was carried out in many small steps, where the initial diameter was 50 mm and the final projection was 15 mm. After processing, the consolidated material was removed from the containment vessel and further subjected to recrystallization annealing in a vacuum furnace at 1200 °C for 4 hours. Attention was paid to the characterization of the microstructure of the material by scanning electron microscopy (SEM). The Vickers hardness was measured to obtain a preliminary assessment of the mechanical properties. Furthermore, attention was paid to cerrp properties, which characterize the creep of the material at elevated temperatures. The CREP was compared with the commercial alloy INCONEL718.

3. RESULTS AND DISCUSSION

3.1. Structural analysis

The microstructures were obtained by SEM (backscattered electron analysis) from the central part of the hot forged RS samples and the dispersion distribution of nano oxides. The microstructure of the grain after RS (**Figure 3**) is coarser in nature. The grain width is around 200 nm and the grains are greatly elongated in the horizontal packing direction. The corrugated swaged structure contains some portion of relatively coarse nanooxides (20-50 nm). For these reasons, the dispersion of nanooxides (**Figure 4**) corresponds to the grain size of hot forming. This structure is characterized by a coarser and less homogeneous grain size distribution. The nano-oxides are mainly formed at the locations of the original grain boundaries. The nanooxides form chains parallel to the horizontal axis.

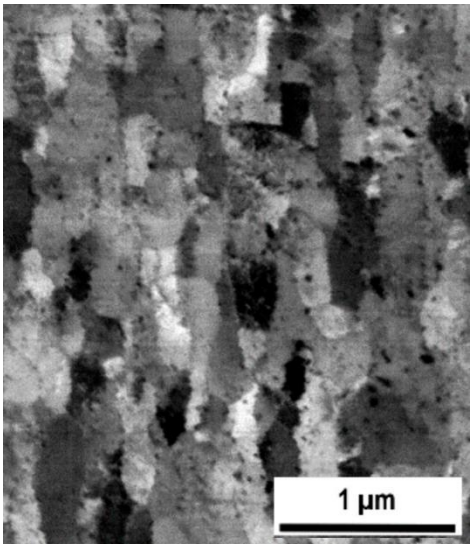

Figure 3 Microstructures prepared by rotary swaging

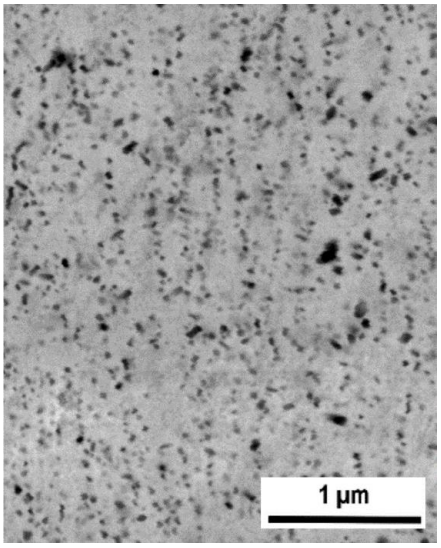

Figure 4 Microstructures of nano-oxide dispersion within grains after aniling

The microstructure after annealing (**Figure 5**) shows a high variance in grain sizes as a function of distance from the sample center in the cross section. The edge is formed by a coarse-grained structure (**Figure 5a**), which varies in grain size in the order of hundreds of microns. The central region of the sample (**Figure 5c**) from about 5 mm in diameter to the center is composed of fine-grained structure with grain sizes in the tens of micrometers, which are surrounded by a large number of ultrafine grains with grain sizes less than 1 µm. This phenomenon is probably due to accumulated plastic deformation after RS, which remained embedded in the structure as a driving force for secondary recrystallization in the central regions.

This is probably one of the reasons why partial recrystallization of the grain microstructure occurred only in the central region. In the longitudinal section, it can be seen that the grains stretch in the longitudinal axis of the blank due to RS processing. The subsequent annealing results in the formation of elongated grains in the axis direction is more marked. Both structures show the same trend in grain size as described for the cross section (**Figures 5b and 5d**).

a) 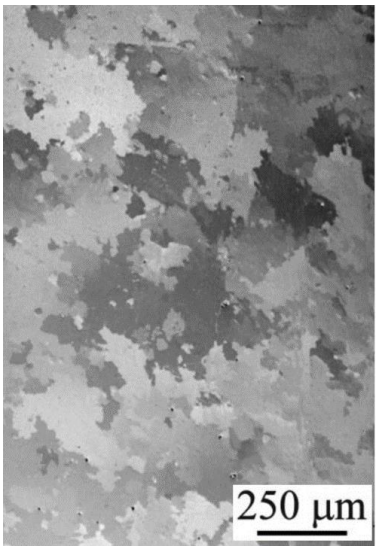

b) 

Figure 5/1 SEM micrographs of the specement after annealing. The coarse-grained rod periphery in the transversal cut (a) and longitudinal cut (b), fine-grained rod core in transversal cut (c) and longitudinal cut (d) together with details in inlets.

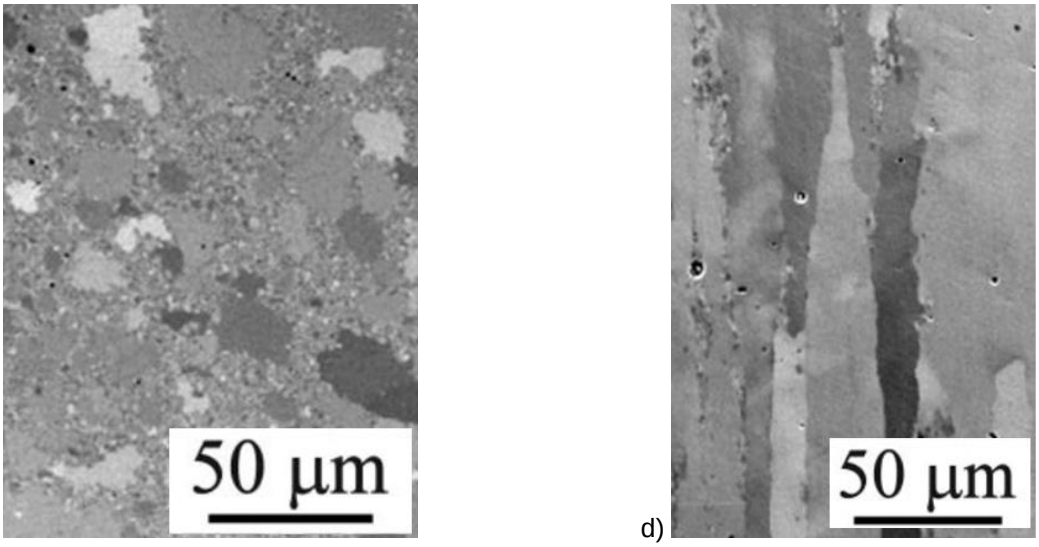

Figure 5/2 SEM micrographs of the specement after annealing. The coarse-grained rod periphery in the transversal cut (a) and longitudinal cut (b), fine-grained rod core in transversal cut (c) and longitudinal cut (d) together with details in inlets.

3.2. Mechanical Testing

Tensile tests carried out at 1100 °C and a strain rate of 10^{-6} s^{-1} showed a strength of 115 MPa and a ductility of 1.2 %. The low ductility and pure intergranular fracture indicated that the cohesive strength at the grain boundary was the weakest point in the samples. This did not play an important role in creep experiments where the applied stress is well below the measured tensile strength.

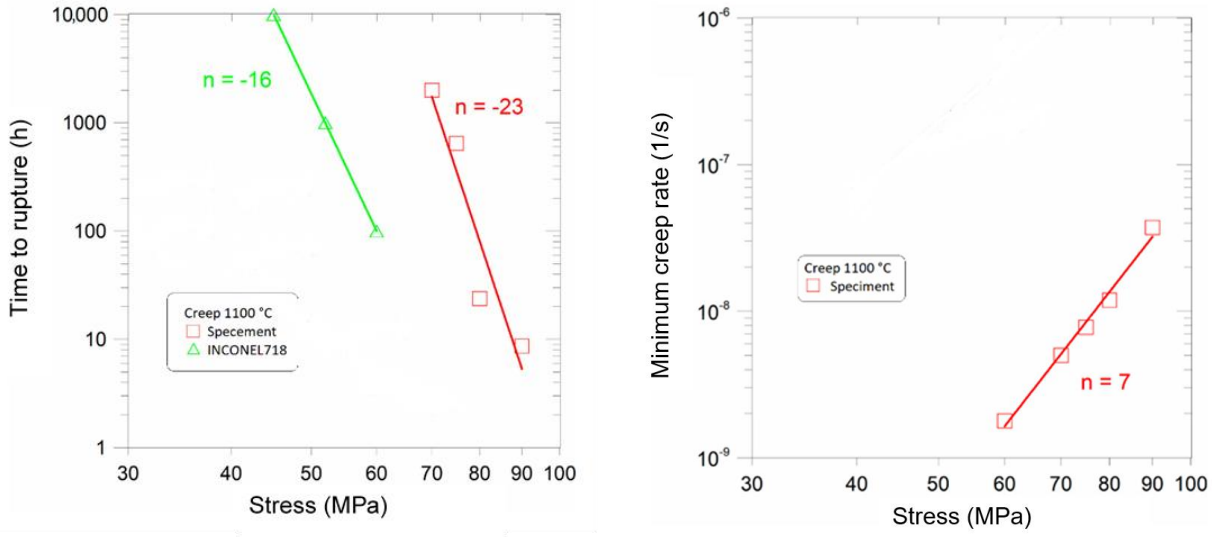

Figure 6 Creep test (**a**) time to rupture; (**b**) minimum creep rate Interrupted creep test of Specimens II at 60 MPa is used to determine the minimum creep rate.

The results of the creep tests conducted at 1100 °C are shown in **Figure 6**. The creep properties of the ODS alloy are compared with the INCONEL718 data sheet. **Figure 6a** clearly shows that the stress exponent of time to break is lower than the commercially produced INCONEL alloy. This can be attributed to the significantly increased creep of the tested ODS alloy at low stress. The stress exponents of the minimum creep rate are

shown in **Figure 6b** for the tested ODS alloy. From the creep tests (**Figure 6a**), it is clear that the strength of the tested specimen is significantly lower than that of the conventional alloy.

4. CONCLUSIONS

- The new generation ODS alloy Fe-10Al-4Cr-4Y2O3 is prepared by mechanical alloying and subsequent consolidation of the powder without air access under heat (at 950 ± 20 °C) by rotary swaging and then recrystallization annealing with the intention of large grain growth.
- Secondary recrystallization is manifested in the central regions of the sample by an ultrafine grained microstructure, while in the surface regions we see a coarse grained structure with significant elongation in the direction of the horizontal axis.
- The creep strength of the ODS alloy at 1100 °C is mainly defined by the morphology of the grain boundaries, which are the weakest point due to their limited cohesive strength.
- The creep strength at 1100 °C of ODS alloys strengthened by rotary hot forging exceeds the commercial INCONEL 718 ODS alloy by more than 30 %.

ACKNOWLEDGEMENTS

This research was supported by the Czech Science Foundation, grant number 17-01641S.

REFERENCES

[1] SVOBODA, J., LUKÁŠ, P. Model of creep in<001>-oriented superalloy single crystals. *Acta Mater.* 1998, vol. 46, pp. 3421–3431.

[2] OKSIUTA, Z. High-temperature oxidation resistance of ultrafine-grained 14% Cr ODS ferritic steel. *J. Mater. Sci.* 2013, vol. 48, pp. 4801–4805.

[3] KUNČICKÁ, L., KOCICH, R., HERVOCHES, C., MCHÁČKOVÁ, A. Study of structure and residual stresses in cold rotary swaged tungsten heavy alloy. *Mater. Sci. Eng. A.* 2017, vol. 704, pp. 25–31.

[4] SVOBODA, J., HORNÍK, V., SRTATIL, L., HADRABA, H., MAŠEK, B., KHALAJ, O., JIRKOVÁ, H. Microstructure Evolution in ODS Alloys with a High-Volume Fraction of Nano Oxides. *Metals*. 2018, vol. 8, pp. 1079.

[5] SVOBODA, J., LUKÁŠ, P. Creep deformation modelling of superalloy single crystals. *Acta Mater.* 2000, vol. 48, pp. 2519–2528.

[6] KUMAR, D., PRAKASH, U., DABHADE, V.V., LAHA, K., SKATHIVEL, Z. Development of Oxide Dispersion Strengthened (ODS) Ferritic Steel Through Powder Forging. *J. Mater. Eng. Perform*. 2017, vol. 26, pp. 1817–1824.

[7] FINTOVA, S., KUBENA, I., LUPTAKOVA, N., JARY, M., SMID, M., STRATIL, L., SISKA, F., SVOBODA, J. Development of advanced Fe-Al-O ODS alloy microstructure and properties due to heat treatment. *J. Mater. Res.* 2020, vol. 35, pp. 2789–2797.

[8] SISKA, F., STRATIL, L. HADRABA, H., FINTOVA, S., KUBENA, I., ZALEZAK, T., BARTKOVA, D. High temperature deformation mechanisms in the 14% Cr ODS alloy. *Materials Science and Engineering a-Structural Materials Properties Microstructure and Processing.* 2017, vol. 689, pp. 34–39.

[9] MACHÁČKOVÁ, A., KRÁTKÁ, L., PETRMICHL, R., KUNČICKÁ, L., KOCICH, R. Affecting structure characteristics of rotary swaged tungsten heavy alloy via variable deformation temperature. *Materials.* 2019, vol. 12, pp. 4200.

[10] CHALUPOVA, A., SULAK, I., SVOBODA, J. High temperature cyclic plastic response of new-generation ODS alloy. *Metals.* 2020, vol. 10, pp. 804.

[11] RÖSLER, J., ARZT, E. A new model-based creep equation for dispersion strengthened materials. *Acta Metall.* 1990, vol. 38, pp. 671–683.